

## MHD Shocks and the Origin of the Solar Transition Region

Margarita Ryutova\* and Theodore Tarbell†

*Lockheed Martin Solar & Astrophysics Laboratories, Palo Alto, California 94304, USA*

(Received 28 June 2002; published 15 May 2003)

Simultaneous observations of the solar atmosphere from its surface to the corona obtained with the Solar and Heliospheric Observatory (SOHO) and Transition Region and Coronal Explorer (TRACE) show a ubiquitous sequence of events that start from cancellation of photospheric magnetic fields, pass through shock formation, and result in transition region supersonic jets and microflares. These results support a novel view of the energy buildup in the solar atmosphere associated with a cascade of shock waves produced by interacting network magnetic elements in the photosphere and provide insight into the origin of the solar transition region. The findings account for the general mechanisms of energy production, transfer, and release throughout the Sun's and stellar atmospheres.

DOI: 10.1103/PhysRevLett.90.191101

PACS numbers: 96.60.Mz, 52.30.-q, 96.50.Fm, 96.60.Na

The sharp temperature jump from the Sun's surface (6000 K) to the  $1 \times 10^6$  degree corona occurs within a narrow transition region which is the site of radiative transients, plasma jets, and explosive events [1–3]. The mechanisms that originate the transition region and determine energy flow in the solar atmosphere involve fundamental physical processes that are commonplace throughout astrophysics and laboratory plasma physics, and yet poorly understood. Recent advances in observations with the SOHO [4] and TRACE [5] spacecraft provided a unique opportunity to compare data taken simultaneously at different heights of the solar atmosphere [6–9].

It was found that there are three main classes of radiative transients that are ubiquitous in the chromosphere-transition region [10–12]: (i) bright localized emissions (“microflares”) not exhibiting significant flows of material; (ii) microflares with lesser intensities, but accompanied by one or two-directional plasma jets: as a rule, stronger microflares correspond to lower velocity jets, and vice versa; (iii) strong supersonic jets and explosive events “alone,” not associated with microflares. Localization of these events in the transition region is cospatial with the photospheric magnetic pattern, and their appearance usually correlates with canceling mixed polarity magnetic elements. In these studies TRACE, Michelson Doppler imager (MDI), and solar ultraviolet measurements of emitted radiation (SUMER) on SOHO were pointed at the same region of quiet Sun near disk center. High resolution magnetograms taken by MDI compiled in a 2.2-h movie showed changes in small scale magnetic elements in the photosphere. These were coaligned with TRACE images (with 15 s cadence) in the C IV lines showing a response of the transition region at temperatures  $\sim 10^5$  K; SUMER provided time series of spectra in C II and O VI lines which correspond to chromospheric ( $\sim 2 \times 10^4$  K) and transition region ( $\sim 3 \times 10^5$  K) temperatures, respectively. An example of coaligned images from these data sets is shown in the left panels of Fig. 1. Analysis of these observations revealed the properties of

transition region jets and microflares consistent with the mechanism of hydrodynamic cumulation associated with shock-shock interaction proposed by Tarbell *et al.* (1999). But the direct observation of shocks and their possible association with photospheric magnetic flux reduction, which would make the theory and interpretation of the observational results decisive, was not available in the above studies.

In this Letter we present the results of observations extended to line profiles of SUMER spectra measured simultaneously with the radiation intensities in the chromosphere-transition region and variation of the magnetic fluxes in underlying photosphere. These results not only reveal the shock signatures and their evolution, but allow us to demonstrate for the first time a direct connection of shocks with the magnetic flux reduction and subsequent appearance of the transition region sporadic events.

The unified mechanism that explains the observed coupling between the photosphere and overlying layers of atmosphere and adequately describes diverse properties of sporadic radiative transients is based on a cascade of shock waves produced by colliding and reconnecting flux tubes in the photospheric network [9,12]. Brought together by convective motions, flux tubes collide and reconnect. Post-reconnection dynamics of the photospheric magnetic flux tubes is radically different from the well-studied case of a low beta coronal plasma, where  $\beta = 8\pi p/B^2 \ll 1$ , and the reconnection liberates a large amount of energy stored in the magnetic field leading to strong *in situ* heating. The photospheric reconnection does not give *in situ* heating. Instead, it sets the system in a highly unsteady state triggering strongly nonlinear processes. These processes occur at a distance from the reconnection area, higher in the atmosphere. This is caused by specific conditions in the photosphere (absent in the corona): (1) concentration of the photospheric magnetic field in small scale, intense magnetic flux tubes, embedded in an almost nonmagnetic environment, and (2) sharp stratification of the low atmosphere. The first

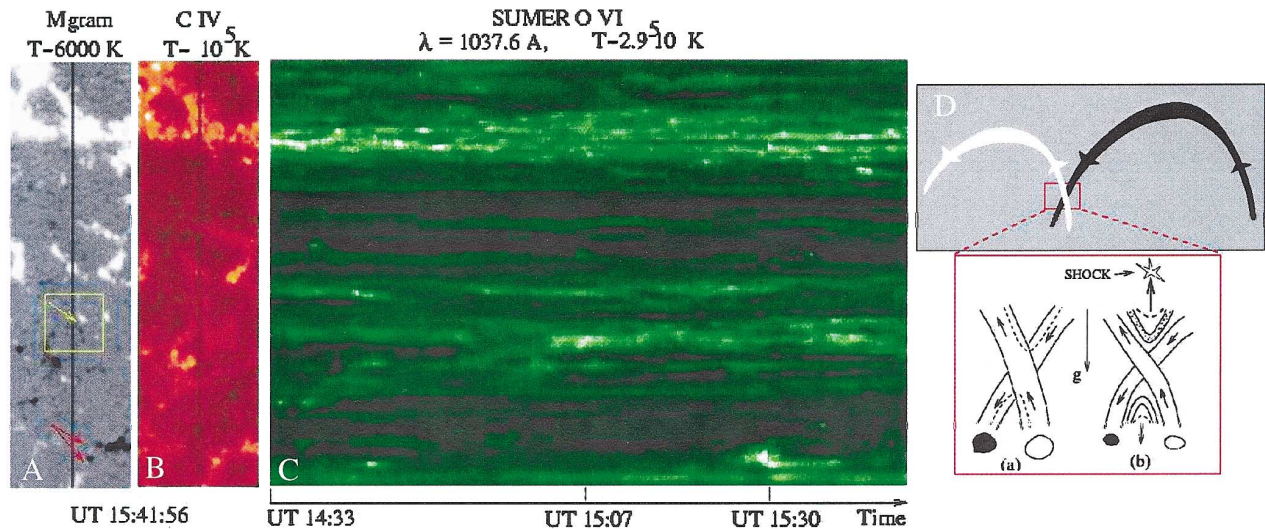


FIG. 1 (color). Left panels: Sample multiwave images of a quiet Sun region near disk center with the angular size of  $66'' \times 220''$  ( $1'' \approx 726$  km). (a) The MDI magnetogram of the studied region: small scale network magnetic elements of positive (white) and negative (black) polarities that outline the regular set of supergranules. (b) The same region at transition region heights: the enhanced emission in C IV line mimics the network magnetic pattern. Solid lines on these images show the SUMER slit position (slit width is  $1''$ ). (c) The time variation of O VI line intensities at each position of the slit during a 75 min time sequence. Each bright dot on this image corresponds to the enhanced plasma flows. Their occurrence also traces closely the sites of magnetic elements. Panel (d): Schematic of two opposite polarity flux tubes brought together by convective motions. The red box shows magnified region of intersection: (a) just before the reconnection, and (b) soon after the reconnection. Black and white spots depict line-of-sight negative and positive magnetic field as seen in the magnetograms. Radii of photospheric flux tubes vary from tens of km up to several hundreds of km. A characteristic radius of magnetic flux tube participating in one elemental act of reconnection is  $\sim 40\text{--}80$  km [11]. This means that magnetic flux tubes having a radius at the MDI resolution limit, i.e.,  $450\text{--}500$  km, are the sites of multiple reconnection processes.

condition implies that the magnetic pressure inside flux tubes,  $B_{\text{tube}}^2/8\pi$ , is always less than the external gas pressure,  $p_{\text{ext}}$ , due to pressure equilibrium,  $p_{\text{ext}} = p_{\text{in}} + B_{\text{tube}}^2/8\pi$ , and the environmental plasma beta is very large,  $\beta = 8\pi p_{\text{ext}}/B_{\text{ext}}^2 \gg 1$ . Therefore, after reconnection, the strongly curved magnetic field lines remain confined in thin flux tubes and behave as elastic bands: straightening they create a sling-shot effect which generates acoustic or MHD waves [Fig. 1, panel (d)]. Most importantly, the atmosphere here is strongly stratified. Because of the sharp stratification those waves that propagate upward in the direction of a decreasing density quickly become shocks [13–15]. Higher in the atmosphere shocks produced by neighboring reconnection processes collide. This leads to hydrodynamic cumulation, i.e., concentration of the energy of a system into a small volume [16] (see also [17] and references therein). Depending on the geometry of shock front convergence, the highly concentrated energy may be either converted entirely into heat or into strong jets, or be distributed between the two. If the shocks experience a head-on collision, immediately after the collision the plasma behind the reflected shocks is at rest, and all the initial kinetic energy is converted into thermal energy of plasma confined in a small volume. Such a process will have the observed signature of a microflare *alone*. If the colliding shocks intersect at some angle, the finite angle between the reflected shocks

gives the plasma space to escape. Therefore, only part of the kinetic energy of the system is converted into heat and part into cumulative jets. With increasing angle of collision more energy goes into plasma jets at the expense of local heating. At some critical angle the entire energy is converted into cumulative jets. The theoretical results for the critical angles of shock front convergence, expressed through the observable quantities (e.g., magnetic field, Mach number, temperature) define the parameter ranges for “HEAT,” “JET,” and “HEAT-JET” regimes [9]. As observed, the largest range of parameters corresponds to the “HEAT-JET” regime where the energy is distributed between the microflares and cumulative jets.

It is important that the radiative transients — microflares and jets — are products of a *shock-shock collision*. Before the shock collision, the regular behind-shock heating occurs, that explains an overall increase of the *background temperature* in the chromosphere and transition region, which is indeed observed to mimic the photospheric magnetic pattern. After collision, behind the reflected shocks additional temperature increase occurs accompanied by a sporadic event having the form of a localized microflare, or highly collimated jets or their combination.

We have analyzed more than 200 different events of bright radiative transients and multiple flows during the 2.2 h observing period. Appearance of each event was

necessarily preceded by reduction of the photospheric magnetic field. A typical example of the analyzed data sets is shown in Fig. 2. The measured magnetic flux reduction, the height where the sporadic event appears, and time of its appearance are consistent with the values calculated from the theory of gradient acceleration of shocks in the stratified atmosphere [12]. Usually the C II ( $T \approx 10^4$  K) shocks are propagating upward and appear soon after the magnetic flux cancellation in the photosphere and before the enhanced emission in hotter C IV ( $T \approx 10^5$  K) and O VI ( $T \approx 3 \times 10^5$  K) lines appears. Figure 3 shows a typical example of the entire process: flux reduction in close bipoles [marked by the white arrow in panel (a)] triggers shock formation in the chromospheric C II line. The difference between the two peaks,  $\Delta\lambda^*$  may be used as a measure of the shock velocity. In its maximum stage  $v_{sh} = 69 \text{ km s}^{-1}$ . At C II temperature ( $2.3 \times 10^4$  K, sound speed  $c_s = 24 \text{ km s}^{-1}$ ) this corresponds to Mach number  $M = v_{sh}/c_s \approx 3$ . At transition region heights such a shock may generate jets (in the HEAT-JET regime, Fig. 2) with velocities ranging from 105 to 170  $\text{km s}^{-1}$  (cf. Eq. (6) in [9]). Fast evolution of the shock [shown in panel (b) in three instances of

time] is followed by the appearance of a bright transient in C IV line and a hot O VI plasma jet. The measured velocity of the jet at  $t = 15:07:10$  is  $118 \text{ km s}^{-1}$ .

An example demonstrating shock-shock interaction is shown in Fig. 4. Reconnections occurring in close bipoles marked by double red arrows in Fig. 1(a) cause a series of upward propagating shocks [Fig. 4(a)]: left peaks are higher than right peaks corresponding to higher intensity behind the shock than in front of it. These shocks result in two close microflares and strong two-directional jets in O VI [right panels in Fig. 4(a)]. The jet generates the downward O VI shock: now the double-humped spectrum has its right peak higher than the left one, which interacts with the upward propagating C II shock at  $t = 15:30:45$  UT [blue line in Fig. 4(b)]. This results in the immediate appearance of the O VI explosive event [marked by yellow arrows in lower right panel of Fig. 4(b)] and a strong C II jet. Prior to the collision temperature increases only due to regular, behind-shock

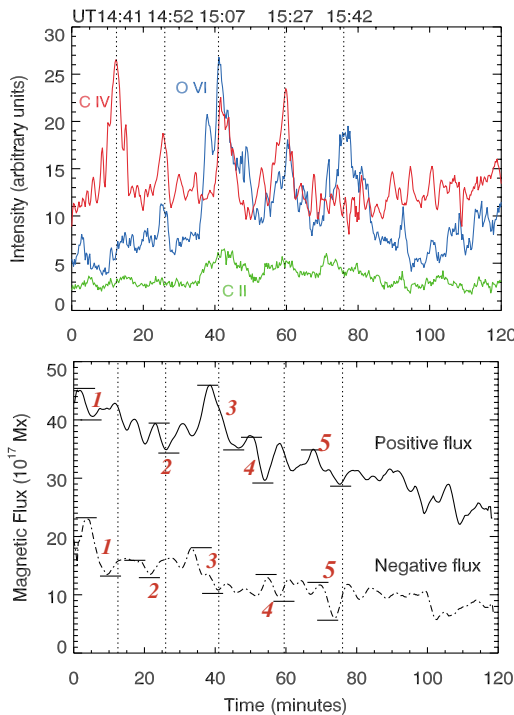


FIG. 2 (color). Time variation of positive and negative magnetic fluxes in the compact bipole inside the yellow box in Fig. 1, and corresponding changes in the C IV (the red line in the upper panel), C II (green line) and O VI (blue line) intensities over this area. The flux reduction marked by “1” in the lower panel caused the appearance of microflare alone without significant flows (a pure “HEAT” regime); the next three events correspond to the “HEAT-JET” regime when microflares are accompanied by the O VI plasma jets, and the event marked by “5” is the example of a pure “JET” regime.

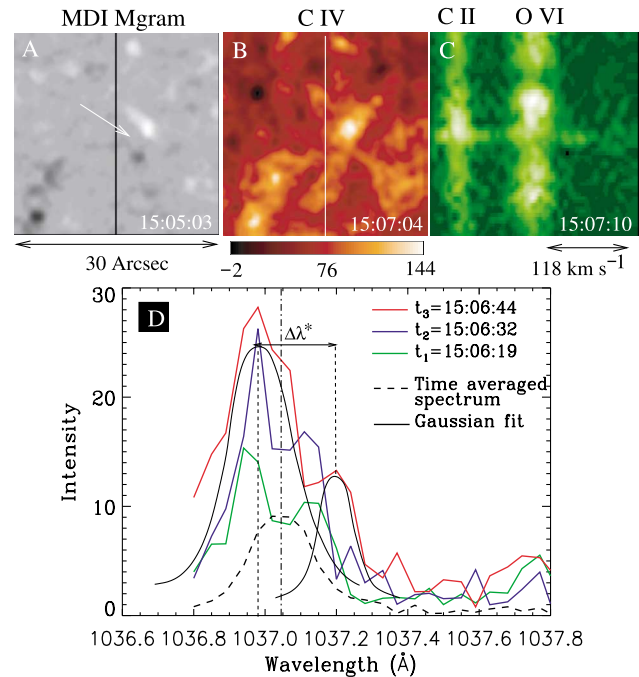


FIG. 3 (color). Key elements of energy production and its release in the chromosphere-transition region associated with the photospheric magnetic flux reduction. (a) Magnetogram of  $30'' \times 30''$  area [yellow square in Fig. 1(a)] with compact bipole near the SUMER slit just before the reconnection occurred. (d) Line profiles of C II SUMER spectra extracted from exposures with 13 sec time step: from  $t_1 = 15:06:19$  (green line) a double-humped profile typical of shocks rapidly evolves into a strong shock (blue and red lines); at its maximum ( $t_3 = 15:06:44$ ) the difference between the two peaks (black solid line is a Gaussian fit),  $\Delta\lambda^* = 0.18 \text{ \AA}$ , which gives for the shock velocity  $v_{sh} = 0.5(\gamma + 1)(v_2 - v_1) = 69 \text{ km s}^{-1}$ , where  $(v_2 - v_1) = c(\Delta\lambda^*/\lambda_0)$ ,  $\lambda_0 = 1037.0 \text{ \AA}$ , and  $\gamma = 5/3$ . This shock caused appearance of a microflare, panel (b), and a strong O VI jet with velocity  $v_{jet} = 118 \text{ km s}^{-1}$ , (c).

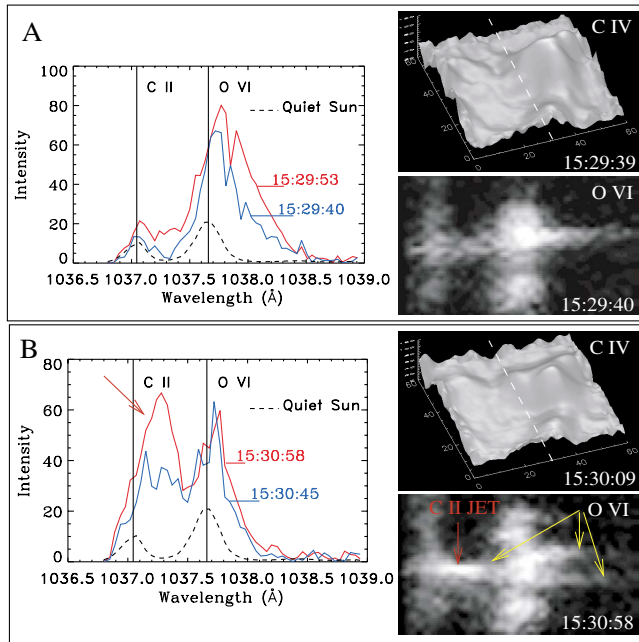


FIG. 4 (color). Sample shock-shock interaction and the resulting sporadic events. (a) A series of strong shocks continuing to occur during and after the double microflare at C IV temperature appeared accompanied by the downward propagating O VI jet (peaks are significantly red-shifted) with velocity exceeding  $180 \text{ km s}^{-1}$ . (b) Downward propagating shocks (O VI line profiles show the right peaks exceeding the left peaks) interact with a series of upward propagating C II shocks at  $t = 15:30:45$ ; the approaching shocks could cause triple humps seen at an earlier moment of time ( $t = 15:30:09$ ) in the C IV line; immediately after the shock collision, at  $t = 15:30:58$  a strong C II jet and the explosive event in O VI line (marked by yellow arrows) appear. The field of view in panels of C IV images and scales of the SUMER spectra are the same as in Fig. 3.

heating,  $T_1 = 2\gamma(\gamma - 1)(\gamma + 1)^{-2}M^2T_0$  (subscripts “0” and “1” denote the unperturbed and behind-shock plasma, respectively). In this example the shock velocity (before the collision) is  $v_{sh} \approx 88 \text{ km s}^{-1}$ , and  $T_1 = 8.5 \times 10^4 \text{ K}$ . After the collision behind the reflected shocks the temperature increases further and becomes  $T_2/T_1 = (3\gamma - 1)\gamma^{-1}$ ,  $T_2 = 2.46 \times 10^5 \text{ K}$ . This is accompanied by strong plasma jets. The jet velocities are in the range of  $115\text{--}220 \text{ km s}^{-1}$ . These are typical observed parameters in the transition region sporadic events.

We conclude that the process that starts from magnetic flux reduction in the photosphere passes through shock formation, then through shock-shock interaction that results in the hydrodynamic cumulation, and ends up in the release of the energy either in the form of the bright radiative transient or plasma jets or combinations of the two, is as ubiquitous as the quiet Sun magnetic network itself. This network covers 90% of the solar surface. Its “recycling” time is very short [18]: in about 40 h magnetic field in the entire network replaces itself providing

continuous energy supply to the upper atmosphere. The energy flux estimated on the basis of this time scale is enough to explain the observed U/EUV radiation of the order of  $5\text{--}10 \times 10^5 \text{ erg cm}^{-2} \text{ s}^{-1}$ . The height of the most intensive shock formation and subsequent appearance of the impulsive phenomena corresponds to the empirical height of the sharp temperature jump. The high rate of emergence of new fluxes and diversity of their parameters result in the cascade of shock waves, thus creating a magnetic energy avalanche and “steady” energy input into higher layers of atmosphere. This is an ongoing process. It works all the time and is independent of the phase of magnetic activity of the Sun. We conclude that permanent energy production from hydromagnetic activity of network magnetic elements is the most natural source for the sharp temperature jump and origin of the unsteady phenomena comprising the chromosphere and transition region.

We would like to thank Robert Becker, Dick Shine and David Alexander for reviewing the manuscript and Phil Judge and Hardie Peter for providing the SUMER data.

\*Also at Lawrence Livermore National Laboratory/ Institute of Geophysics and Planetary Physics, L-413, Livermore, CA 94550.

†Electronic address: ryutova@llnl.gov

- [1] O. Kjeldseth-Moe *et al.*, *Astrophys. J.* **334**, 1066 (1988).
- [2] K. P. Dere, J.-D. F. Bartoe, and G. E. Brueckner, *Sol. Phys.* **123**, 41 (1989).
- [3] J. T. Mariska, *The Solar Transition Region* (Cambridge University Press, Cambridge, United Kingdom, 1992).
- [4] Special Issue on the SOHO Mission, edited by B. Fleck, V. Domingo, and A. I. Poland [*Sol. Phys.* **162**, Nos. 1–2 (1995)].
- [5] B. N. Handy *et al.*, *Sol. Phys.* **187**, 229 (1999).
- [6] R. A. Harrison *et al.*, *Sol. Phys.* **170**, 123 (1997).
- [7] P. Brekke, D. M. Hassler, and K. Wilhelm, *Sol. Phys.* **175**, 349 (1997).
- [8] D. E. Innes, P. Brekke, D. Germerott, and K. Wilhelm, *Sol. Phys.* **175**, 341 (1997).
- [9] T. Tarbell, M. Ryutova, J. Covington, and A. Fludra, *Astrophys. J.* **514**, L47 (1999).
- [10] M. P. Ryutova and T. D. Tarbell, *Astrophys. J.* **541**, L29 (2000).
- [11] T. Tarbell, M. Ryutova, and R. Shine, *Sol. Phys.* **193**, 195 (2000).
- [12] M. P. Ryutova, S. R. Habbal, R. Woo, and T. Tarbell, *Sol. Phys.* **200**, 213 (2001).
- [13] L. D. Landau and E. M. Lifshitz, *Fluid Mechanics* (Pergamon Press, Oxford, 1987).
- [14] G. B. Whitham, *J. Fluid Mech.* **3**, 337 (1958).
- [15] Pai Shih-I, *Magnetogasdynamics and Plasma Dynamics* (Springer-Verlag, New York, 1962).
- [16] K. P. Stanyukovich, *Unsteady Motion of Continuous Media* (Pergamon Press, Oxford, 1960).
- [17] I. V. Sokolov, *Sov. Phys. Usp.* **33**, 960 (1990).
- [18] C. J. Schrijver, *et al.*, *Astrophys. J.* **487**, 424 (1997).